Middle East Journal of Applied Sciences
Volume: 13 | Issue: 04| Oct. – Dec. | 2023

EISSN: 2706 -7947 ISSN: 2077- 4613
DOI: 10.36632/mejas/2023.13.4.34
Journal homepage: www.curresweb.com
Pages: 523-537

Integration of Geospatial Techniques for Flood Hazards Detection in Wadi Atfih, Eastern Desert, Egypt

Mona M. M. Omar

Hydrology Department, Desert Research Center, Egypt

Received: 15 Sept. 2023 **Accepted:** 20 Oct. 2023 **Published:** 30 Oct. 2023

ABSTRACT

Combining geospatial techniques (remote sensing and GIS techniques) with the Analytical Hierarchy Process (AHP) can provide a promising tool for flood risk detection. Therefore, this study aimed to use advanced remote sensing and geospatial techniques combined with the Analytical Hierarchy Process (AHP) to detect flood risks in Wadi Atfih, Eastern Desert Egypt, to produce a flood risk map (FRM). Therefore, multi-sensor remote sensing data from ASTER, Landsat-8, the Shuttle Radar Topography Mission (SRTM), the Tropical Rainfall Measurement Mission (TRMM), and Radarsat-1 were used to construct several geospatial thematic layers. These layers (variables) include elevation, slope, drainage density, topographic moisture index, accumulated precipitation, land use and land cover (LULC), and distance from the river. The Analytical Hierarchy Process (AHP) method was adopted to calculate the weight of the previous variables in addition to the soil type layer to produce the FRM map. This map is categorized into 3 categories, from high to low flood risk. Based on the results, geospatial techniques combined with the analytical hierarchy process can provide a powerful tool for flood risk detection in arid and semi-arid lands and can thus be applied in regions with similar conditions.

Keywords: Analytical hierarchy process; Eastern desert; Geospatial techniques; Flood Risk map; Wadi Atfih

1. Introduction

A model to assess the spatial distribution of flood-prone areas was created by integrating the AHP method with the Geographic Information System in the flood hazard evaluation process (Astutik *et al*., 2021). A Geographic Information System and a multi-criteria decision-making method were integrated with an analytical hierarchy process to identify and map flood-prone areas in the Dega Damot district, in northwest Ethiopia (Negese, 2022). Remote sensing, GIS, and AHP technologies are useful integrated tools for defining a small watershed management plan with a community-based perspective toward development and planning (Bera *et al*., 2023). The capacity to evaluate both qualitative and quantitative criteria simultaneously is offered by AHP. This strategy is a useful tool, especially when choosing among multiple candidates needs to be made (Esen, 2023). Remote sensing data along with geospatial techniques can provide a powerful tool for groundwater probabilities in arid lands and thus can be applied in regions with similar conditions, such as the Middle East countries (Zein El-Din et. al., 2018). Integrated remote sensing and a geophysical approach to assess the flash flood hazards and water infiltration into aquifers in the Wadi Atfih (El-Saadawy *et al*., 2020). The development of aquifer productivity and the mitigation of groundwater quality degradation are strongly recommended in the Atfih area (El-Sayed *et al*., 2018). Studied the effect of the morphological parameters on the surface runoff in Wadi Atfih Using the Davis and Ranking methods of morphological parameters (Omar, 2023).

Compared to conventional methods that analysis of morphological parameters to assess flash flood hazards the combination of geospatial techniques (remote sensing and GIS techniques) with the Analytical Hierarchy Process (AHP) can provide a promising tool for detecting flood hazards. Therefore, the present work relied basically on optical, radar, and thermal remote sensing data and infiltration rate tests for mapping of hazard degrees of the wadi Atfih. The data types were selected to represent the physiographic influence (variables) on flooding hazard. The adopted methodology utilized

Corresponding Author: Mona M. M. Omar, Hydrology Department, Desert Research Center, Egypt.
E-mail: omona5468@gmail.com

EISSN: 2706 -7947 ISSN: 2077- 4613 *DOI: 10.36632/mejas/2023.13.4.34*

the weighted index overlay analysis technique for computing the variables' weights and producing the FRH map. These variables were extracted from remotely sensed data to make the proper integration between them to detect the flooding hazard sites. The workflow for the utilized data and methods consists of two main procedures; first, variables extraction using the compiled remote sensing data products and infiltration rate, and second, product of the flood risk map.

2. Study area

The Wadi Atfih catchment extends from the south of Greater Cairo in the north to the Beni Suef Governorate in the south. It is located in the northern part of the Egyptian Eastern Desert, and lies between longitudes 29°10' and 29°30'E and latitudes 31°10' and 32°00'N, occupying an area of about 468 km^2(Fig. 1a). Stream order of the Wadi Atfih is fifth order (Fig. 1b).

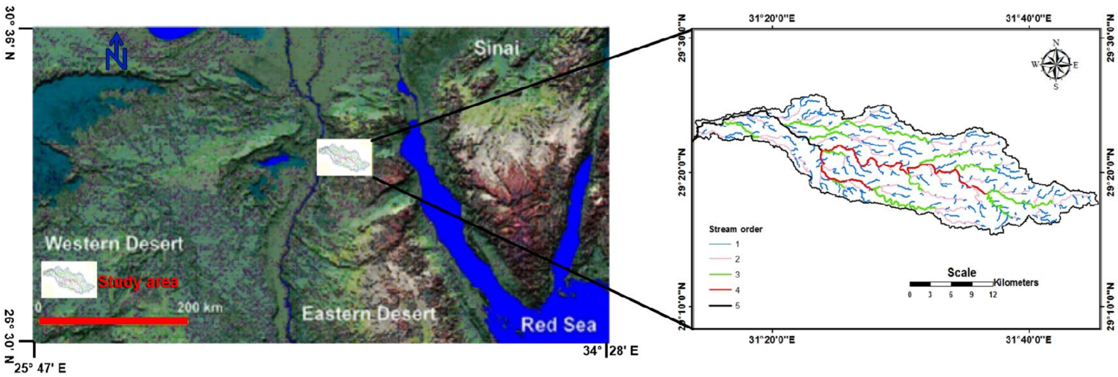

Fig. 1: (a) Study area; and (b) Drainage Map of the Wadi Atfih, Eastern Desert, Egypt.

Geologically, according to Korany *et al.,* (1997), the study area is mainly covered by Tertiary sedimentary rocks (Middle Eocene and Pliocene) and Quaternary alluvium. The Middle Eocene rocks occupy the upstream and midstream areas, built of densely bedded limestone with local cherts and fine nummulites (Mokattam Group unit). Pliocene rocks include undifferentiated sedimentary deposits, including the Kom El Shelul Formation. The Quaternary alluvium occupies the downstream and delta parts. It is built of unconsolidated gravel, sand, silt and clay intercalations. It is recharged by rainfall during the occasional storms and lateral inflow from the connected aquifers in the neighbouring basins and the Nile River (Fig. 2).

Geomorphologically, according to Korany *et al.,* (1997), three main geomorphological units comprise the Wadi Atfih: the structural plateau (Gebel El-Galaa El Baharia), which borders the ancient alluvial plain to the west and is covered by Tertiary carbonaceous rocks. This unit is situated between 300 and 600 metres above sea level. The second unit is the former alluvial plain, situated between 90 and 300 metres above sea level and having a sand and gravel combination covering its surface. This plain has recently been reclaimed for farming, and weathering processes are rife in the exposed rock units. Its terrain is made up of gently sloping sand plains that generally slope westward into the alluvial plain that is still developing. The low-lying relief and the River Nile flood plain compose the third unit, which is the young alluvial plain. Its elevation varies from 16 to less than 90 metres above sea level. The Quaternary sediments, which are primarily made up of unconsolidated sands and gravels, cobbles, and limestone pebbles, cover it, together with a thin layer of silty clay (Fig. 3).

Hydrogeologically, the Quaternary aquifer is the main aquifer in the study area. The groundwater depth ranges from 4 m to 50 m, while the groundwater level ranges from 12.18 m to 44 m (a.m.s.l.). The average discharge rate of the producing wells ranged from 43.56 to 288 m^3/hour. The average pumping hours for the producing wells in the study area ranged from 12 hours in the summer to 8 hours in the winter. Total dissolved solids (TDS) in the Quaternary aquifer range from 582 to 2854.4 ppm in the study area. During a rainstorm that the Wadi Atfih

During a rainstorm that the Wadi Atfih experienced in March 2020, the average volume of runoff and recharge into the Quaternary aquifer was 3.05 million cubic meters and 2.13 million cubic meters, respectively (Omar, 2023).Faiad (1996) reports that for the Quaternary aquifer in Wadi Atfih, the values of transmissivity (T) range from 3657 to 4546.4 m^2/day, whereas the values of storage coefficient (S) range from 3.537 x 10^{-4} to 5.2 x 10^{-4}. This suggests that the aquifer has a low capacity for storage and good potential to transport water through it.

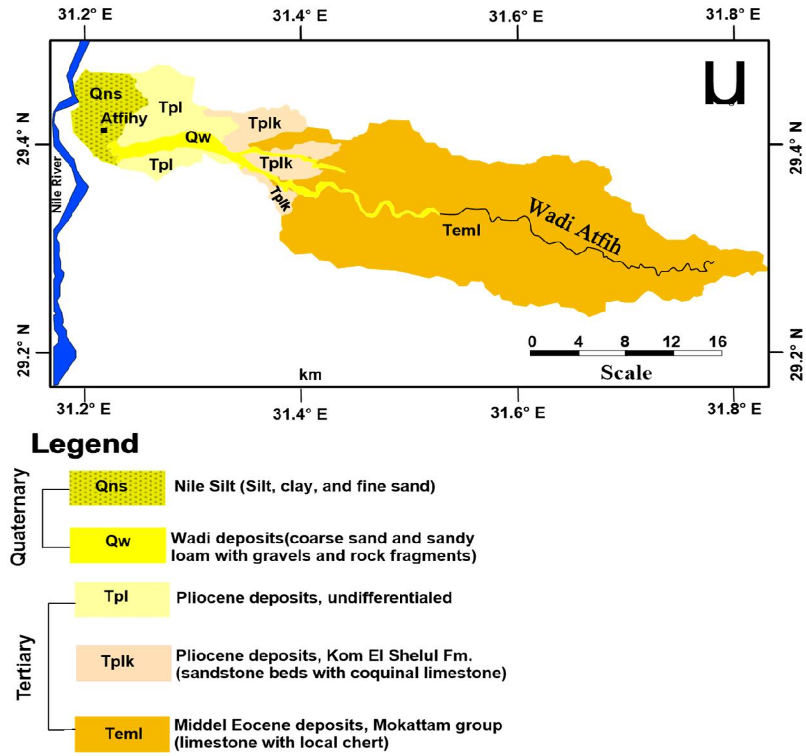

Fig. 2: Geology Map of the Wadi Atfih, Eastern Desert, Egypt (modified from CONOCO, 1987).

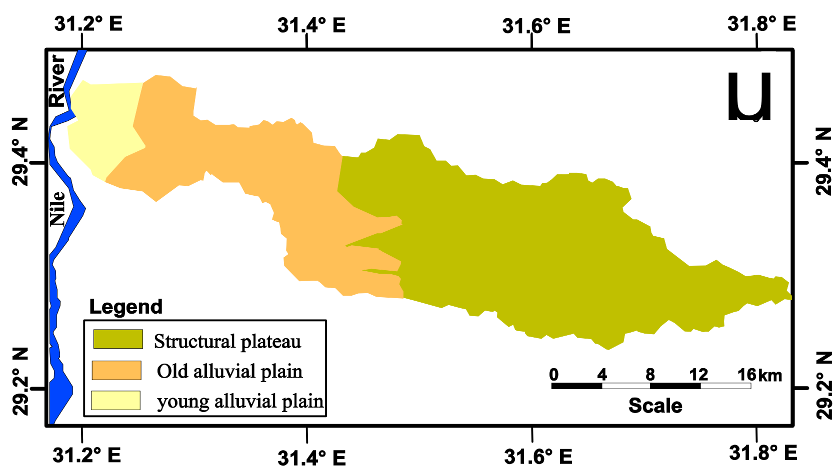

Fig. 3: Geomorphological map of the Wadi Atfih, Eastern Desert, Egypt.

3. Methodology

The integration of geospatial techniques and the Analytical Hierarchy Process (AHP) was used to identify and map potential flood-prone areas in the study area. GIS and remote sensing techniques were used to collect data to prepare layers of elevation, slope, distance to rivers, rainfall, drainage density, topographic moisture index (TWI) and land use land cover (LULC). While the qualitative layer of soil was prepared by conducting infiltration rate experiments that were conducted in the field during the research and also analyzed by the author. Next, using information systems techniques, spatial data layers were created for the previous eight factors influencing the likelihood of floods in a raster format. Once all flood control factors were prepared in raster format, all raster factor maps were reclassified to a spatial resolution of 10 meters using the Resample tool for data management tools in an ArcGIS environment. All raster factor maps were then reclassified using the Spatial Analysis Tools reclassification tool to a common measurement scale from 1 (very low flood susceptibility) to 5 (very high flood susceptibility). After reclassifying all flood control factor maps, the analytical hierarchy process (AHP) model was applied to assign the relative influence weight of each factor. In the end, a flood risk map for the region was extracted by overlaying the eight layers that affect spatial flooding using the weighted overlay method in the ArcGIS environment (Fig.4).

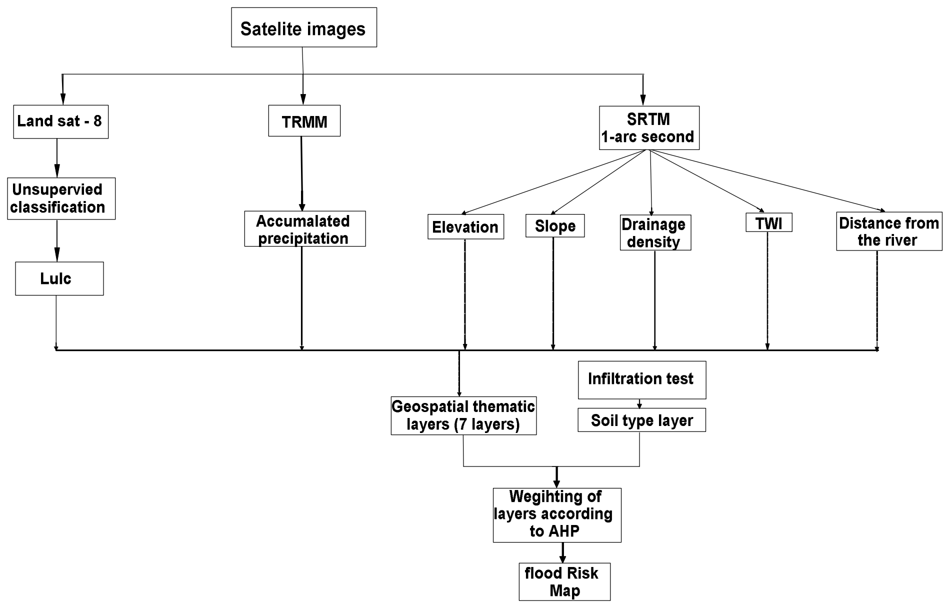

Fig. 4: Flow chart showing the data and methods adopted in the present study.

3.1. Determine the Factors of Flood Conditioning.

According to the workflow in Fig. 4, the adopted methodology includes two stages (1) The construction of the required thematic layers; and (2) Analyzing the FloodRisk Map (FRM) using the AHP method.

3.2. Construction of the Required Thematic Layers

Eight thematic layers (variables) were extracted from satellite data including elevation, slope, drainage density, Topographic Wetness Index (TWI), accumulated precipitation, Land Use/Land Cover (LULC), and distance from the river. The eighth layer is the layer of soil type, which was produced from the analysis of the infiltration rate test during the field. These variables will be mentioned in detail in the following sections:

3.2.1. Digital elevation model

A digital elevation model (DEM) is a digital representation of surface terrain. A DEM model of the study area was created using GIS software from the Shuttle Radar Topography Mission (SRTM) with a grid spacing of 1 arc second (30 m). DEM is essential for producing the mapping of the slope, the drainage network, the drainage density, the distance from the river, and the Topographic Wetness Index (TWI). The elevation of the study area ranges between 16 and 646 m (Fig. 5a).

3.2.2. Slope

The slope is the most important index for delineating and characterizing surface runoff and liable area to FRH due to its indication of the variation in elevation and its right impact on catchments, speed of runoff, and infiltration capabilities (Waqas *et al*., 2021; Yarriyan *et al*., 2020). The slope classes with fewer degrees were assigned a higher grade to FRH, as areas of the lower slope are more exposed to flooding (Ullah *et al*., 2021; Liuzzo *et al.,* 2019; Rahman *et al.,* 2019). Flat areas have a high potential for flooding. However, several studies have implemented positive relationships between slope and flood susceptibility (Abdelkareem *et al.,* (2017; Masoudian *et al.,* 2009; Bapalu *et al.,* 2014). Since the slope angle values increase, the overland flow velocity increases (Tehrany *et al.,* 2014). With increasing the slope degree, the infiltration decreases; hence, there are a larger number of drained streams, creating flooding (Zhu *et al.,* 2021). Therefore, in areas with steep slopes, runoff increases (Benjmel *et al.,* 2020). Based on SRTM DEM, the slope degree map ranges from (0–15) to < 65 (Fig. 5b). In this approach, the slope classes with high degrees were assigned a higher grade for flat flood susceptibility.

3.2.3. Drainage density

Drainage density is computed as the total length per unit area of the stream network. It is negatively correlated to permeability; areas with high Dd are related to surface runoff (Zhu *et al.,* 2021; Mukherjee *et al.,* 2020). Drainage density is positively correlated with flooding; the higher susceptibility to flooding is directly correlated with higher drainage density, as it indicates a high surface runoff (Elkhrachy *et al.,* 2015; Paulet al 2019; Islam *et al.,* 2020; Sharma *et al.,* 2021). The drainage density in the study area ranges from 0–2.1 to 8.6–11 m/km (Fig. 5c).

3.2.4. Topographic Wetness Index (TWI)

The topographic wetness index (TWI) is widely used in fields such as hydrology, geomorphology, ecology, and soil sciences to identify areas with high or low hydrological potential and to identify potential erosion and sedimentation problems. TWI also indicates the effect of flow direction and flow accumulation at a location in the watershed; the higher its value, the more vulnerable watershed for flooding, and vice versa (Das, 2018). It is calculated using GIS as follows:

$$TWI = \ln (a / \tan b) \quad (1)$$

Where:
a: is the specific catchment area (the total area contributing runoff to a particular location)
b: is the local slope of the terrain, measured in radians

The raster of TWI was generated using the aforementioned equation calculated using the SRTM DEM of the study area in the Arc GIS environment. The resulting TWI in the study area ranges between 2.7 to 23 (Fig. 5d).

3.2.5. Land Use and Land Cover (LULC)

Land Use and Land Cover (LULC) generally refers to the categorization or classification of human activities and natural elements on the landscape within a specific time frame based on established scientific and statistical methods of analysis of appropriate source materials. It is significant for mapping the variation in soil types and anthropogenic activities in the plain area, which is critical for runoff infiltration. The study area classified Lucl into 5 classes: waterbody, agriculture, scrub, built-up area, and bare ground (Fig. 5e).

3.2.6. Accumulated Precipitation

The Tropical Rainfall Measurement Mission (TRMM) was used to estimate accumulated precipitation. TRMM is a joint mission between NASDA (Japan National Aerospace Development Agency) and NASA Goddard Space Flight Center dedicated to measuring precipitation in tropical and subtropical regions. Hence, TRMM was used here to estimate the amount of precipitation that occurred between 2011 and 2021. After converting TRMM data from NetCDF format to vector points, the point vectors were interpolated back into interpolated rasters using the spline method. These rasters were then clipped and adjusted to fit the study area (Fig. 5f).

3.2.7. Distance from the river

Distance from the river affects the moisture content of soils and rocks on slopes (Miraki *et al.,* 2019). These factors can affect the recharging process; compared to further distances from river

Middle East J. Appl. Sci., 13(4): 523-537, 2023
EISSN: 2706 -7947 ISSN: 2077- 4613 *DOI: 10.36632/mejas/2023.13.4.34*

networks, the closer the distance to the river, the greater the chance of infiltration. Based on the DEM of the study region in the study area, the distance from the river ranges from (0–100) to less than 900 m (Fig. 5g).

3.1.8. Infiltration rate

The infiltration rate is defined as the volume flux of water flowing into the profile per unit of surface soil area. The experiences of permeability can be utilized in many fields. For example, in areas of flooding or surface runoff, infiltration tests can be used to determine places of high permeability to identify proper locations for retarding dams that work for aquifer recharge. Places with low permeability can be chosen as surface tanks to collect rainwater for agricultural purposes.Due to the wide extension of the investigated area and the good representation of infiltration tests, four infiltration tests were carried out in different locations, representing the different soil units in the studied area. The values of the infiltration rate range from 0.056 to 5.27 m/day. According to Kohnke's (1980) classification, the investigated soil of Wadi El Atfih is characterized by slow, moderate, and rapid rates (Fig. 5k).

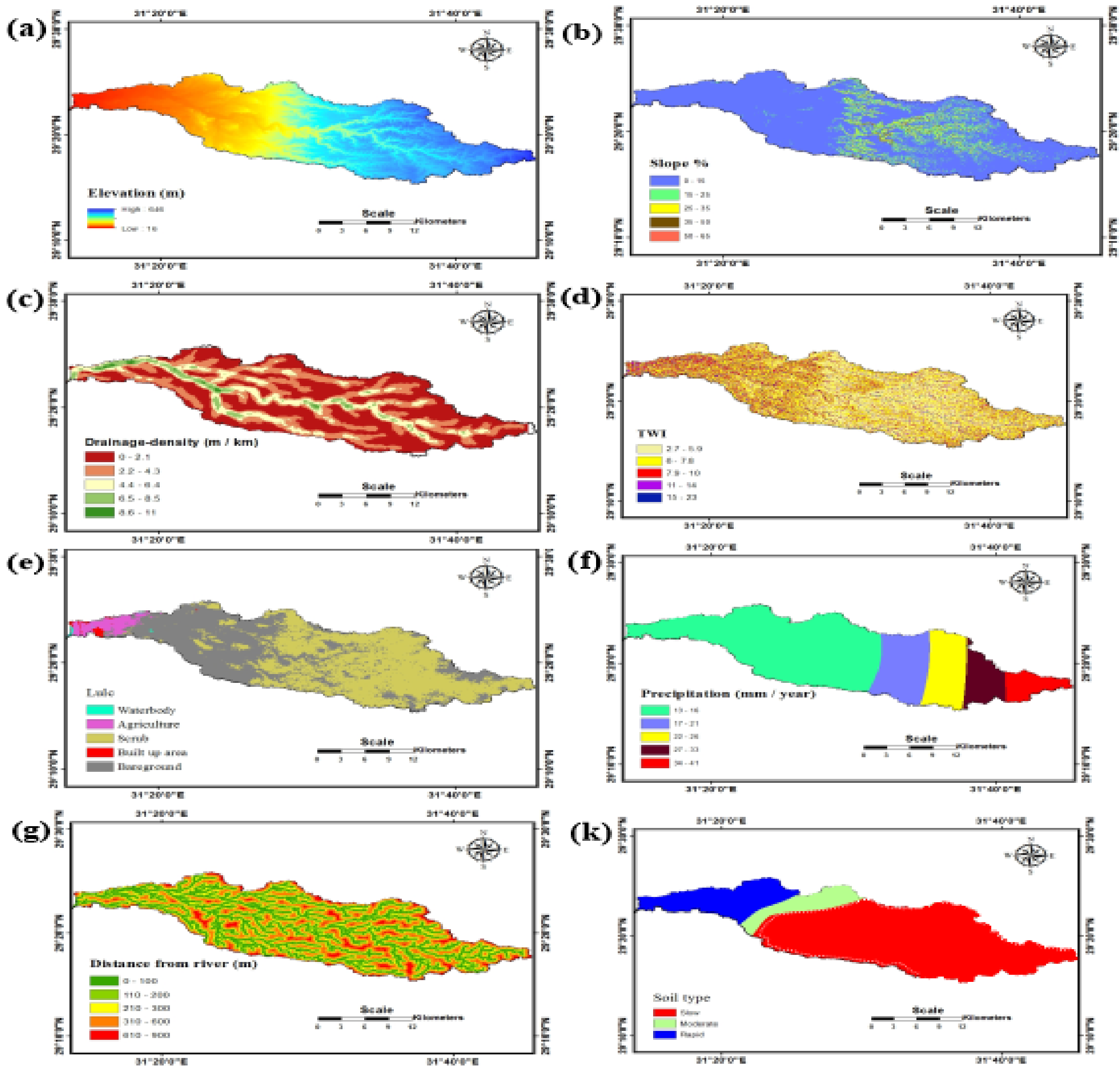

Fig. 5: Factors for flood risk map: (a) Elevation; (b) Slope; (c) Drainage density; (d) TWI; (e) Lulc, (f) Preciptation; (g) Distance from the river; and (k) Soil Type

3.2. Analytical Hierarchy Process (AHP)

The most well-liked and effective technique in multi-criteria decision-making (MCDM) for determining the relative importance of each factor considered in a study is the Saaty Analytical Hierarchy Process (AHP), developed in 1987. This method has been applied in numerous prior studies to identify and map flood-prone areas, as well as to weight each flood control factor (Abdelkarim *et al.,* 2020; Ajibade *et al.,* 2021; Allafta and Opp 2021; Astutik *et al.,* 2021; Aydin and Birincioğlu 2022; Danuma *et al.,* 2016; Das and Gupta 2021; Karimbalis *et al.,* 2021; Mahmoud and Gan 2018; Ogato *et al.,* 2020). Factors used for flood susceptibility mapping using multi-criteria decision-making are given weights based on the evaluation of previous studies and the local physical characteristics of the study area. The following steps were used to assign relative weights to each flood control factor used in this study, according to Saaty (1987):

1. Based on the relative importance, a value ranging from 1 to 9 was assigned to each factor to construct the pairwise comparison matrix (Table 1). According to the scale, 1 refers to equal importance, and 9 refers to extreme importance.
2. Next, using the software of Goepel Version 15.09, 2018, the normalized pairwise comparison matrix table and the weight of each factor were computed.

Table 1: Scale for pair-wise comparison.

Assigned value	Definition	Explanation
1	Parameters are of equal importance	Two parameters contribute equally to the objective
3	Parameter j is of weak importance compared to parameter i	Experience and Judgment slightly favor parameter i over j
5	Essential or strong importance of parameter i compared to j	Experience and Judgment strongly favor parameter i over j
7	Demonstrated importance	Criteria i is strongly favored over j and its dominance is demonstrated in practice
9	Absolute importance	The evidence favoring parameter i over j to the highest possible order of affirmation
2,4,6 & 8	Intermediate values between two adjacent judgmen	Judgment is not precise enough to assign values of 1,3,5,7,and 9

After the computation of weights for each flood-controlling factor, the consistency check was performed using the equations given below to check whether the comparison is correct or consistent. The consistency index (CI) is calculated using the following equation (Eq. 2) as given by Saaty (1987).

$$\mathbf{CI} = \frac{\lambda\text{max} - \text{n}}{\mathbf{n-1}} \quad \text{......(2)}$$

Where λmax represents the principal eigenvalue of the matrix, and n is the number of variables in the matrix.Finally, the consistency ratio (CR) was computed using the following equation (Eq. 3) suggested by Saaty (1987) to verify the consistency of the comparison.

$$\mathbf{CR} = \frac{\text{CI}}{\mathbf{RI}} \quad \text{......(3)}$$

Where CR is the consistency ratio, CI is the consistency index, and RI is the random index, which varies according to the number of factors used in the pairwise comparison. If the CR is below 0.10, it means that the pairwise comparison matrix has acceptable consistency. Otherwise, if the CR is greater than or equal to 0.10, it means that pairwise comparison has inadequate consistency, and the comparison process must be repeated until the value of CR is achieved below 0.10 (Saaty 1987).

4. Results and Discussion

It is pointless to perform the flood risk map directly on the extracted thematic layers without a weighted index connecting them based on their hazard degrees. Therefore, all raster factor maps were reclassified to a common measurement scale from 1 (very low) to 5 (very high) using the Reclassify tool of Spatial Analyst tools and rescaled to 10 m spatial resolution using the Resample tool of Data Management Tools in the ArcGIS environment.

Floods occur due to several topographic and climatic factors in an area. The influence of each factor is undoubtedly different and will produce an overview of locations prone to various levels of flooding. In this study, eight variables influence the occurrence of flooding, which will then be modeled using the Analytical Hierarchy Process (AHP). Each of these variables will be discussed in detail below:

4. a. Elevation

One of the factors used to assess flood risk is elevation. Generally, lower elevated areas have a higher probability of flood occurrences compared to higher elevated areas because lower elevated areas have comparatively higher wadi discharge and get flooded faster by the flow of high water (Hong *et al.,* 2018a, b; Lee and Rezaie, 2022; Zzaman *et al.,* 2021). The altitude of the study area ranges from 16 to 646 m above sea level. As shown in Fig. 6a, areas with low elevation, which are located in the western part of the study area (altitude below 16 m above sea level), are the most vulnerable areas to flood inundation. On the other hand, areas with central parts have low and moderate susceptibility to flooding. About 15.42% and 21.72% of the study area have a very high and high susceptibility to flooding, respectively (Table 2).

4. b. Slope

The slope of the land controls the velocity of surface water flow. As the slope decreases, the velocity of surface water flow decreases, and the amount of water over the land and the probability of a flood increase (Astutik *et al.,* 2021; Das and Gupta, 2021; Zzaman *et al.,* 2021). Yariyan *et al.,* (2020) considered slopes from 0 to 15, 15 to 30, 30 to 45, 45–60, and >60 degrees as having very high, moderate, low, and very low susceptibility to floods, respectively. The reclassified slope map (Fig. 6b) shows that about 84.13% of the study area has a slope range from 0 to 15 degrees, which belongs to a very high susceptibility to flooding. About 11.39 and 3.72% of the study area are characterized by high (15–25°) and moderate (25°–35°) susceptibility to flooding, respectively. Areas of low (35–50°) and very low (60–65°) flood susceptibility cover about 0.72% and 0.04%, respectively (Table 2).

4. c. Accumulated Precipitation

The consideration of rainfall as a factor in flood susceptibility analysis is a must since we cannot think about flood occurrence without it. It is the most crucial triggering factor for the occurrence of floods because flood inundation is due to a huge volume of runoff flows as a result of excessive heavy rainfall or prolonged rainfall (Allafta and Opp 2021; Hong *et al.,* 2018a,b). The mean annual rainfall of the district varies from 13 to 41 mm/year and is reclassified (13–16 mm), (17–21 mm), (22–26 mm), (27–33 mm), and (34–41 mm) as a very low, low, moderate, high, and very high contribution to flooding, respectively. As shown in Fig. 6c, the eastern parts of the study area are the most susceptible parts to flood inundation compared to the western parts. About 5.92%, 8.41%, 13.42%, 15.89%, and 56.35% of the study areas were classified as very high, high, moderate, very low, and low vulnerability to flooding, respectively (Fig. 6c, and Table 2).

4. d. Distance from the river

Areas that are close to rivers have a higher probability of flood inundation than areas located far away from the rivers since surplus water from the rivers initially reaches alongside river banks and adjoining lowland areas (Mahmoud and Gan 2018). This is because as the distance increases, the slope and elevation become higher (Lee and Rezaie, 2022; Zzaman *et al.,* 2021). In the study area, areas that are within a distance of 0-100 m from the river are categorized as very highly susceptible to flooding, while areas within a distance from the river (110-200, 210-300, 310-600, and 610-900 m) are considered to have a high, moderate, low, and very low vulnerability to flooding, respectively (Fig. 6d and Table 2).

4. e. Drainage density

Surface runoff and the probability of flooding increase with drainage density (Abdelkarim *et al.,* 2020; Das and Gupta, 2021; Lee and Rezaie, 2022; Mahmoud and Gan, 2018).The drainage density value in this study is classified into five categories: very low (0.14–1.35 km/km^2), low (1.35.4–2.55

km/km^2), moderate (2.55–3.76 km/km^2), high (3.76–4.9 km/km^2), and very high (4.9 km/km2–6.17 km/km^2). About 3%, 13%, 28%, 38%, and 18% of the study area were classified as having very high, moderate, very low, and low vulnerability to flooding, respectively (Table 2 and Fig. 6e).

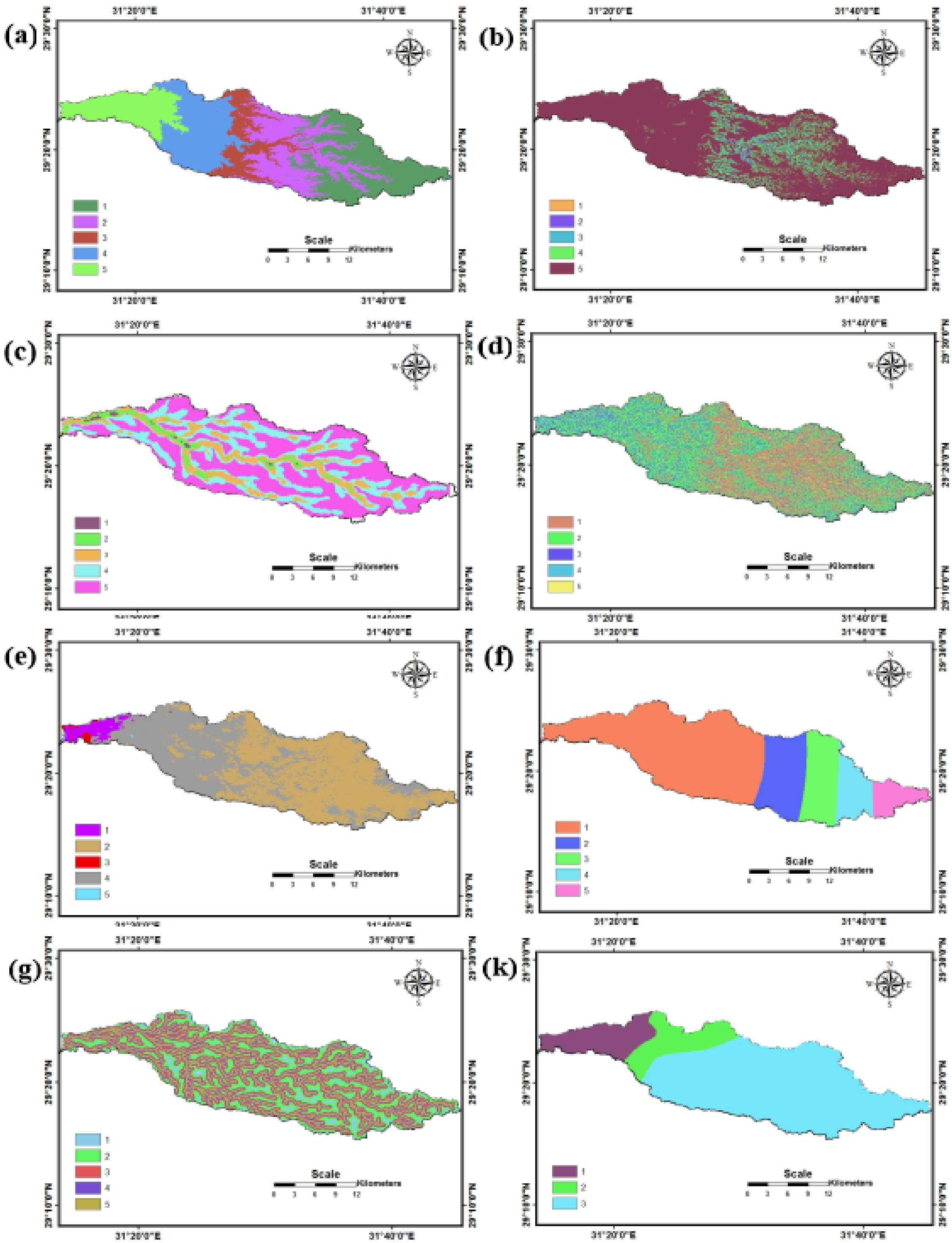

Fig. 6: Reclassification of flood – contoring factor (a) Elevation; (b) Slope; (c) Drainage density; (d)TWI; (e) Lulc, (f) Preciptation; (g) Distance from the river; and (k) Soil Type.

Middle East J. Appl. Sci., 13(4): 523-537, 2023
EISSN: 2706 -7947 ISSN: 2077- 4613 *DOI: 10.36632/mejas/2023.13.4.34*

Table 2: Pairwise comparison matrix for selected flood controlling factors

	Drainage density	Slope	Elevation	Distance from to river	Infiltration rate	Topographic wetness index	Precipitation	Land use / land cover
Drainage density	1	2	2	2	2	4	4	4
Slope	0.5	1	1	1	1	2	2	2
Elevation	0.5	1	1	1	1	2	2	2
Distance from to river	0.5	1	1	1	1	2	2	2
infiltration rate	0.5	1	1	1	1	2	2	2
Topographic wetness index	0.25	0.5	0.5	0.5	0.5	1	1	1
Precipitation	0.25	0.5	0.5	0.5	0.5	1	1	1
Land use / land cover	0.25	0.5	0.5	0.5	0.5	1	1	1

4. f. Topographic wetness index (TWI)

The Topographic Wetness Index is an index used to quantify the topographical effect on runoff generation and flow accumulation volume at any given place. It depicts the tendency of water to collect at a given spot or travel downhill due to gravitational pressure (Lee and Rezaie, 2022). The Topographic Wetness Index is capable of predicting areas susceptible to saturated land surfaces and areas that carry the potential to produce overland flow (Hong *et al.,* 2018a, b). The TWI is directly proportional to flood risk; the higher the TWI value, the greater the likelihood of flood inundation (Das and Gupta 2021). A study conducted by Ali *et al.,* (2020) considered areas with a TWI of 5.57 to 7.58, 7.58 to 8.68, 8.68 to 10.17, 10.17 to 12.63, and 12.63 to 22.09 as having very low, low, moderate, high, and very high susceptibility to flooding, respectively. Likewise, as shown in Fig. 6f and Table 2, the TWI of the study area was classified into five classes of susceptibility to flooding: very low (2.7–5.9), low (6–7.8), moderate (7.9–10), high (11–14), and very high (15–23), which covers 31.99%, 42.17%, 15.81%, 7.74%, and 2.29% of the study area, respectively.

4. g. Land use and land cover (LULC)

One of the most important factors in flood occurrence is land use and land cover. Because vegetation slows the rapid flow of water and induces high infiltration, areas with a high density of vegetation are often less vulnerable to flood risk. In urban and residential areas, on the other hand, runoff increases due to impermeable surfaces and little infiltration (Allafta and Opp 2021; Das and Gupta 2021; Kazakis *et al.,* 2015; Zzaman *et al.,* 2021). Das and Gupta (2021) categorized waterbody, build-up, agriculture, sparse vegetation, and dense vegetation as having very high, moderate, low, and very low vulnerability to flooding, respectively. Hagos *et al.,* (2022) also classified built-up areas, farmland, grassland, shrubland, and forestland areas as having extremely high, moderate, low, and extremely low vulnerability to flooding, respectively. Likewise, the LULC map of the study area is categorized as having very high (water body), high (bare ground), moderate (built-up area), low (scrub), and very low (vegetation) susceptibility to floods. Scrub and bare ground are the major LULC types of the district, covering about 52.27% and 43.41%, respectively, of the study area (Fig. 6g and Table 2), and representing low susceptibility to flooding. Vegetation, built-up area, and water body are about 3.66%, 0.53%, and 0.13%, respectively.

4. k. Soil types

Nyarko (2002) and Todini *et al.,* (2004) report that soil type and texture play a role in determining the water holding and infiltration characteristics of an area and consequently affect flood susceptibility. The soil type layer for the study area has been classified into three classes of susceptibility to flooding: low, moderate, and high, which covers 13.01% (60.89 km^2), 12.96% (60.65 km^2), and 74.03% (346.46 km^2) of the study area, respectively (Fig. 6k and Table 2).

4.2. Analytical hierarchy process (AHP) analysis

AHP analysis was performed to determine the relative weight or influence of flood-controlling factors subject to a weighted overlay after each flood-controlling factor was reclassified (Fig. 6). A pairwise comparison matrix was developed (Table 2), and the normalization of the pairwise comparison and the weight of the factors were computed (Table 3). The result of the consistency ratio (CR) calculation is 0.00. The CR value is still below the value of 0.10; the weighting is accepted and can be analyzed further for the subcategories of each factor. The contribution of each class in determining the flood hazard area is described in Table 3. The factors of drainage density, slope, elevation, TWI, lulc, precipitation, and distance from the river are divided intofive classes, while soil type is divided into three classes. Class 1 is the class that has the least effect on flooding, and class 5 is the class that has the most influence on flood events.

Table 3: Classes of the factors and according weights

Factor layer	Weight (W) (Priority)	Detailed Features/Sub-Classes	Rank	Area (%)	Area km^2
Drainage density	17%	0.14 - 1.35	1	3	14.04
		1.35 - 2.55	2	13	60.84
		2.55 - 3.76	3	28	131.04
		3.76 - 4.96	4	38	177.84
		4.96 - 6.17	5	18	84.24
Slope	10%	0 - 15	1	0.04	0.19
		15 -30	2	0.72	3.37
		30 - 45	3	3.72	17.41
		45 - 60	4	11.39	53.31
		> 60	5	84.13	393.73
Elevation	12%	16 - 132	5	27.65	129.40
		132 - 247	4	23.35	109.28
		247 - 375	3	11.85	55.46
		375 - 480	2	21.72	101.65
		480 - 646	1	15.42	72.17
Distance from the river	14%	0 - 100	5	5.37	25.13
		110 - 200	4	29.61	138.57
		210 - 300	3	18.89	88.41
		310 - 600	2	20.22	94.63
		610 - 900	1	25.91	121.26
Infiltration rate	15%	slow	4	13	60.84
		Moderate rapid	3	12.96	60.65
		rapid	2	74.03	346.46
Topographic wetness index	9%	2.7 - 5.9	1	31.99	149.71
		6 - 7.8	2	42.17	197.36
		7.9 - 10	3	15.81	73.99
		11.1 - 14	4	7.74	36.22
		15 - 23	5	2.29	10.72
Precipitation	9%	13 - 16	1	56.35	263.72
		17 - 21	2	15.89	74.37
		22 - 26	3	13.42	62.81
		27 - 33	4	8.41	39.36
		33 - 41	5	5.92	27.71
Land use and land cover	14%	Vegatation	1	3.66	17.13
		Scrub	2	52.27	244.62
		Built up area	3	0.53	2.48
		Bareground	4	43.41	203.16
		Waterbody	5	0.13	0.61

4.3. Flood Risk Map of the study area

After all, flood-control factor maps had been reclassified. The analytical hierarchy process (AHP) model was used to assign a relative weight of influence to each factor. The final risk flood map of the district was derived by overlaying the eight flood-controlling spatial layers using the weighted overlay method in the ArcGIS environment. The Analytical Hierarchy Process (AHP) classified the district into three flood susceptibility classes: high (4) 21.9% (101.56Km^2), moderate (3) 78.05% (365.27 Km^2), and low (2) 0.05% (1.17 Km^2) susceptibility. In general, 78.05% of the total watershed area is under moderate hazards (Fig. 7 and Table. 4).

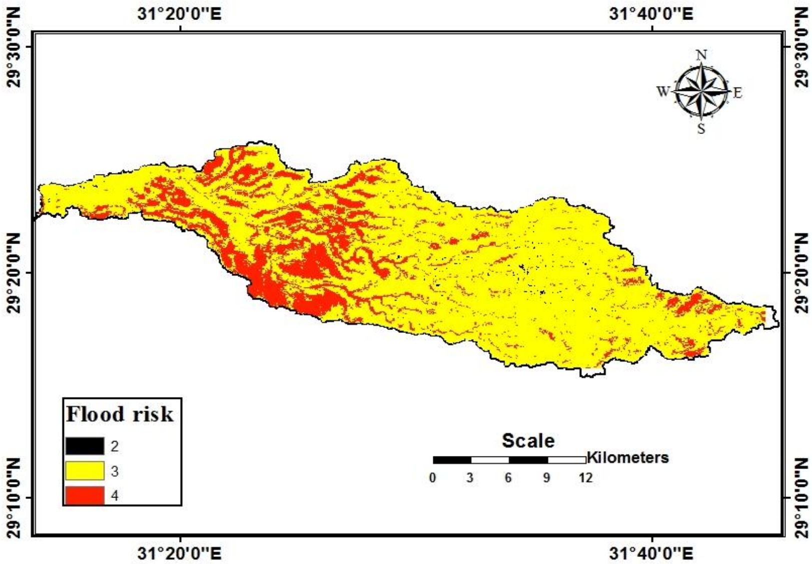

Fig. 7: Flood risk map, Wadi Atfih, Eastern Desert, Egypt.

Table 4: Areas according to the level of flood susceptibility

Flood Hazard Classes	Area	
	km^2	%
Low	1.17	0.05
Moderate	365.27	78.05
High	101.56	21.9
Total	468	100.00

5. Conclusion

This study integrates remote sensing data and geospatial techniques for mapping flood risk in one promising location for development in the Eastern Desert, which is Wadi Atfih. The importance of utilizing remote sensing data instead of conventional land-based techniques was to produce continuous surface maps at higher resolutions and consistent scales than previously published maps. Therefore, the main objective of this work is to use advanced remote sensing and geospatial techniques combined with the Analytical Hierarchy Process (AHP) to detect flood risks in Wadi Atfih, Eastern Desert Egyp, and produce a flood risk map (FRM). A wide range of remote sensing data, including optical, radar, and thermal sensors, was used to construct several geospatial thematic layers (variables).

These variables include elevation, slope, drainage density, topographic wetness index, accumulated precipitation, land use and land cover (LULC), and distance from the river. While the soil type layer was prepared by conducting infiltration rate experiments that were conducted in the field during the research and also analyzed by the author, all variables were arranged and weighted based on their flood susceptibility. The Analytical Hierarchy Process (AHP) method was adopted for computing the weights of variables and producing the FRM. The FRM indicates that most of the total watershed area in Wadi Atfih (78.05%) is subject to moderate flood hazards. While 21.9% is subject to high flood hazards, in conclusion, the present study shows that geospatial techniques combined with the analytical hierarchy process can provide a powerful tool for flood risk detection in arid and semi-arid lands and can thus be applied in regions with similar conditions.

References

Abdelkarim, A., S.S. Al-Alola, H.M. Alogayell, S.A. Mohamed, I.I. Alkadi, and I.Y. Ismail, 2020. "Integration of GIS-based multicriteria decision analysis and analytic hierarchy process to assess food hazards on the Al-Shamal train pathway in Al-Qurayyat region, Kingdom of Saudi Arabia." Water. https://doi.org/10.3390/w12061702

Abdelkareem, M., 2017. "Targeting flash flood potential areas using remotely sensed data and GIS techniques." Nat. Hazards J. 85: 19–37. [CrossRef]

Ajibade, F.O., T.F. Ajibade, T.E. Idowu, N.A. Nwogwu, B. Adelodun, K.H. Lasisi, O.T. Opafola, O.A. Ajala, O.G. Fadugba, and J.R. Adewumi, 2021. "Flood-prone area mapping using GIS-based analytical hierarchy frameworks for Ibadan city, Nigeria." J Multi-Criteria Decis Anal. 28(5–6):283–295. https://doi.org/10.1002/mcda.1759

Ali, S.A., F. Parvin, Q.B. Pham, M. Vojtek, J. Vojtekova, R. Costache, N.T.T. Linh, H.Q. Nguyen, A. Ahmad, and M.A. Ghorbani, 2020. "GIS-based comparative assessment of flood susceptibility mapping using hybrid multi-criteria decision-making approach, naive Bayes tree, bivariate statistics, and logistic regression: A case of Topľa basin, Slovakia." Ecol. Indic. https://doi.org/10.1016/j.ecolind.2020.106620

Allafta, H., and C. Opp, 2021. "GIS-based multi-criteria analysis for food-prone area mapping in the trans-boundary Shatt Al-Arab basin, Iraq-Iran. Geomat Nat Haz Risk" 12(1):2087–2116. https://doi.org/ 10.1080/19475705.2021.1955755

Astutik, S., E.I. Pangastuti, E.A. Nurdin, F.A. Ikhsan, F.A. Kurnianto, B. Apriyanto, and M.A. Mujib, 2021. "Assessment of Flood Hazard Mapping Based on Analytical Hierarchy Process (AHP) and GIS: Application in Kencong District, Jember Regency, Indonesia." Geosfera Indonesia. https://doi.org/10.19184/geosi.v6i3.21668.

Aydin, M.C., and S.E. Birincioğlu, 2022. "Flood risk analysis using the gis-based analytical hierarchy process: a case study of Bitlis Province." Appl. Water Sci. https://doi.org/10.1007/s13201-022-01655-x Binns, AD (2022) Sustainable development and food risk management. J. Flood Risk Management. https://doi.org/10.1111/jfr3.12807

Bapalu, G.V., and R. Sinha, 2005. "GIS in Flood Hazard Mapping: A Case Study of Kosi River Basin, India." Available online: https://www.researchgate.net/profile/Rajiv-Sinha2/ publication /200004867 GIS_ in_ Flood _Hazard _Mapping _a_case_ study_of_ Kosi_ River_ Basin_ Indialinks/ 0046353bd6f9186023000000/ GIS-in-Flood-Hazard-Mapping-a-case-study-of-KosiRiver-Basin-India.pdf (accessed on November 8, November2014).

Benjmel, K., F. Amraoui, S. Boutaleb, M. Ouchchen, A. Tahiri, and A. Touab, 2020. "Mapping of groundwater potential zones in crystalline terrain using remote sensing, GIS techniques, and multicriteria data analysis (case of the Ighremregion, western Anti-Atlas, Morocco)." Water 2020, 12, 471 [CrossRef]

Blaschke, T., 2020. "Flood susceptibility mapping using an improved analytic network process with statistical models." Geomat Nat Haz Risk 11(1):2282–2314. https://doi.org/10.1080/4775705. 2020. 18360 36

CONOCO, 1987. " Geological map of Egypt, scale 1: 500000, sheet." No. N.H. 36 sw Beni Suef, the Egyptian General Petrleum Corporation

Das, S., 2018. "Geographic information system and AHP-based flood hazard zonation of Vaitarna basin, Maharashtra, India." Arabian Journal of Geosciences, 11 (19). https://doi.org/10.1007/s12517-018-3933-4.

Das, S., and A. Gupta, 2021." Multi-criteria decision-based geospatial mapping of food susceptibility and temporal hydro-geomorphic changes in the Subarnarekha basin, India." Geosci Front. https://doi.org/10.1016/j.gsf.2021.101206

Elkhrachy, I., 2015. "Flash Flood Hazard Mapping Using Satellite Images and GIS Tools: A Case Study of Najran City, Kingdom of Saudi Arabia (KSA), Egypt." J. Remote Sens. Space Sci. 2015, 18, 261–278. [CrossRef]

El-Saadawy, O., A. Gaber, A. Othman, A.Z. Abotalib, M. El Bastawesy, and M. Attwa, 2020. "Modeling flash floods and induced recharge into alluvial aquifers using multi-temporal remote sensing and electrical resistivity imaging," Sustainability by J. of MDPI, 12, 10204; doi: 10.3390/su122

El-Sayed, S.A., S.M. Morsy, and K.M. Zakaria, 2018. "Recharge sources and geochemical evolution of groundwater in the Quaternary aquifer at Atfih area, the northeastern Nile Valley, Egypt." J. Afr. Earth Sci. 142: 82–92. [CrossRef]

Esen, H., 2023. Analytical Hierarchy Process Problem Solution as a chapter in the book citation index, IntechOpen, Creative Commons Attribution, (http://creativecommons.org/licenses/by/3.0)

Faiad, B.J., 1996. "Hydrogeological Studies of the Groundwater Systems in the Quaternary Aquifer, Wadi El-Atfihy, Eastern Desert, Egypt." M. Sc. Thesis. Fac. Sci. AinShams Univ., Cairo, Egypt, 300

Hong, H., P. Tsangaratos, I. Ilia, J. Liu, A.X. Zhu, and W. Chen, 2018b. "Application of fuzzy weight of evidence and data mining techniques in the construction of a flood susceptibility map of Poyang County, China. Sci Total Environ 625:575–588. https://doi.org/10.1016/j. scito tenv. 2017. 12. 256

Islam, M.M., and K. Sado, 2000. "Flood hazard assessment in Bangladesh using NOAA AVHRR data with geographical information system." Hydrol.Process. 2000, 14: 605–620. [CrossRef]

Karymbalis, E., M. Andreou, D.V. Batzakis, K. Tsanakas, and S. Karalis, 2021. "Integration of GIS-based multicriteria decision analysis and analytic hierarchy processes for flood-hazard assessment in the Megalo Rema River Catchment (East Attica, Greece)" Sustainability. https://doi.org/10.3390/su131-810232

Kohnke, H., 1980. "Soil Physics", Soil Scientists, Purdue University, TataNc Grow-Hill Publishing Company LTD, New Delhi, 28–34.

Korany, E.A., M.M. El-Ghazawi, and B.J. Faiad, 1997. "Hydrographic analysis and hydrogeologic bearing of Wadi El-Atfihy, Eastern Desert, Egypt—a case study of an ephemeral stream." Ain Shams Science Bulletin, 35: 73–88

Lee, S., and F. Rezaie, 2022. "Data used for GIS-based flood susceptibility mapping." Data Geol Ecol Oceanogr Space Sci Polar Sci., 41:1–15. https://doi.org/10.22761/ DJ2022. 4.1. 001

Liuzzo, L., V. Sammartano, and G. Freni, 2019. "Comparison between Different Distributed Methods for Flood Susceptibility Mapping." Water Resour. Manag. 33: 3155–3173. [CrossRef]

Mahmood, S., and R. Atta-ur, 2019. "Flash flood susceptibility modeling using geo-morphometric and hydrological approaches in Panjkora Basin, Eastern Hindu Kush, Pakistan." Environ. Earth Sci. 78, 43 [CrossRef]

Mahmoud, S.H., and T.Y. Gan, 2018. "Multi-criteria approach to developing food susceptibility maps in arid regions of the Middle East." J. Clean Prod., 196:216–229. https://doi.org/10.1016/j.jclepro.2018.06.047

Masoudian, M., 2009. "The Topographical Impact on Effectiveness of Flood Protection Measures." Ph.D. Thesis, Faculty of Civil Engineering, Kassel University, Kassel, Germany, 2009. Available online: https://books.google.co.jp/books?hl=zh-TW&lr=&id= uc15e5ukEC &oi=fnd&pg=PA72&dq=The+opographical+Impact+on+Effectiveness+of+Flood+Protection+ Measures.+Ph.D.Thesis.+Faculty+of+Civil+Engineering,+Kassel+University:+Kassel,+Germany,+2009&ots=f-N5ezRQFV&sig=nOMXpD6Fr0yR42qe BCZdIPxS9M#v =onepage &q&f =false (Accessed on December 10, 2013).

Miraki, S., S.H. Zanganeh, K. Chapi, V.P. Singh, A. Shirzadi, H. Shahabi, and B.T. Pham, 2019. "Mapping groundwater potential using a novel hybrid intelligence approach." Water Resour. Manag., 33: 281–302. [CrossRef]

Mukherjee, I., and U.K. Singh, 2020. "Delineation of groundwater potential zones in a drought-prone semi-arid region of East India using GIS and analytical hierarchical process techniques." Catena, 194: 104681. [CrossRef]

Negese, A., D. Worku, A. Shitaye, and H. Getnet, 2022. "Potential food-prone area identification and mapping using GIS-based multi-criteria decision-making and analytical hierarchy processes in Dega Damot district, northwestern Ethiopia" Applied Water Science, 12:255. https://doi.org/10.1007/s13201-022-01772-7.

Nyarko, B.K. 2002. “Application of a rational model in GIS for flood risk assessment in Accra.” J. Spat. Hydrol., 2(1):1–14.

Ogato, G.S., A. Bantider, K. Abebe, and D. Geneletti 2020. "Geographic information system (GIS)-based multicriteria analysis of flooding hazards and risks in Ambo Town and its watershed, West Shoa Zone, Oromia Regional State, Ethiopia." J. Hydrol Reg Stud., https://doi.org/10.1016/j.ejrh.2019.100659

Omar, M.M., 2023. Impact of morphometric parameters on surface runoff in Wadi Atfih, Eastern Desert, Egypt." IOSR Journal of Applied Geology and Geophysics (IOSR-JAGG) e-ISSN: 2321–0990, p-ISSN: 2321–0982, 11(4) I (July–August 2023), 24-39 www.iosrjournals.org

Paul, G.C., S. Saha, and T.K. Hembram, 2019. "Application of the GIS-Based Probabilistic Models for Mapping the Flood Susceptibility in Bansloi Sub-basin of the Ganga-Bhagirathi River and Their Comparison." Remote Sens. Earth Syst. Sci. 2: 120–146. [CrossRef]

Rahman, M., C. Ningsheng, M.M. Islam, A. Dewan, J. Iqbal, R.M.A. Washakh, and T. Shufeng, 2019. "Flood Susceptibility Assessment in Bangladesh Using Machine Learning and Multi-criteria Decision Analysis. Earth Syst. Environ. 3: 585–601. [CrossRef]

Saaty, W.A., 1987. "The analytic hierarchy process—what and how it is used." Math. Modell., 9(3-5):161–176.

Sharma, T.P.P., J. Zhang, N.R. Khanal, F.A. Prodhan, L. Nanzad, D. Zhang, and P.A. Nepal, 2021. "Geomorphic Approach for Identifying Flash Flood Potential Areas in the East Rapti River Basin of Nepal. ISPRS Int. J. Geo-Inf. 10, 247. [CrossRef]

Tehrany, M.S., B. Pradhan, and M.N. Jebur, 2014. "Flood susceptibility mapping using a novel ensemble weights-of-evidence and support vector machine models in GIS. J. Hydrol. 512: 332–343. [CrossRef]

Todini, F., T. De Filippis, G. De Chiara, G. Maracchi, M.L.V. Martina, and E. Todini, 2004. "Using a GIS approach to assess flood hazards at the national scale." Presentation presented in European Geosciences Union, 1st General Assembly, Nice, France, 25–30.

Ullah, K., and J. Zhang, 2020. "GIS-based flood hazard mapping using the relative frequency ratio method: A case study of Panjkora River Basin, eastern Hindu Kush, Pakistan." PLoS ONE, 15, e0229153. [CrossRef]

Waqas, H., L. Lu, A. Tariq, Q. Li, M.F. Baqa, J. Xing, and A. Sajjad, 2021. "Flash Flood Susceptibility Assessment and Zonation Using an Integrating Analytic Hierarchy Process and Frequency Ratio Model for the Chitral District, Khyber Pakhtunkhwa, Pakistan." Water, 13, 1650 [CrossRef]

Yariyan, P., S. Janizadeh, T. Van Phong, H.D. Nguyen, R. Costache, H. Van Le, B.T. Pham, B. Pradhan, and J.P. Tiefenbacher, 2020. "Improvement of Best First Decision Trees Using Random Subspace and Dagging Ensembles for Flood Probability Mapping." Water Resour. Manag. 34: 1–17. [CrossRef]

Yariyan, P., M. Avand, R.A. Abbaspour, A. Torabi Haghighi, R. Costache, O. Ghorbanzadeh, S. Janizadeh, and M.Y. Zein El-Din, M. AbuBakr, R.G. Hroun, and M.M. Ali 2018. “Integration of Geospatial Techniques for Mapping Groundwater Potentialities in El-Qaa Plain, Southwest Sinai, Egypt, Al Azhar Bulletin of Science, 29(2): 125–142.

Zein El-Din,AbuBakr,M. Y.M., Hroun,R. G., and Ali, M.M. 2018 “Integration of geospatial techniques for mapping groundwater potentialities in El-Qaa PLain, Southwest Sinai, Egypt”
Al Azhar Bulletin of Science Vol. 29, No. 2 (December), 2018, pp. 125-142.

Zhu, Q., and M. Abdelkareem, 2021. “Mapping groundwater potential zones using a knowledge-driven approach and GIS analysis” Water,13, 579 [CrossRef]

Zzaman, R.U., S. Nowreen, M. Billah, and A.S. Islam, 2021. “Flood hazard mapping of the Sangu River basin in Bangladesh using multi-criteria analysis of hydrogeomorphological factors.” J. Flood Risk Management https://doi.org/10.1111/jfr3.12715